American Mineralogist, Volume 93, pages 22–30, 2008

Chemical and physical transfers in an ultramafic rock weathering profile: Part 1. Supergene dissolution of Pt-bearing chromite

Daouda Traoré,[1,2] Anicet Beauvais,[1,2,*] François Chabaux,[3] Chantal Peiffert,[4] Jean-Claude Parisot,[1,2] Jean-Paul Ambrosi,[2] and Fabrice Colin[1,2]

[1]Institut de Recherche pour le Développement (IRD), UMR 161 CEREGE, BP A5, 98848 Nouméa, New Caledonia
[2]Centre Européen de Recherche et d'Enseignement des Géosciences de l'Environnement, (UMR CNRS 6635/UMR IRD 161), Aix-Marseille Université, Université Paul Cézanne, BP 80, 13545 Aix en Provence Cedex 4, France
[3]EOST-Centre de Géochimie de la Surface (CNRS/ULP), Université Louis Pasteur, 1 rue Blessig, 67084 Strasbourg Cedex, France
[4]UMR G2R/CREGU, Université Henri Poincaré 54506 Vandoeuvre-lès-Nancy, France

Abstract

Chemical weathering and supergene dissolution processes of Pt-bearing chromite have been studied in a lateritic weathering profile developed on ultramafic rocks in New Caledonia (southwest Pacific). The chemical distributions of alkaline earth, transition metals, and precious metals (including Pt and Pd) were determined in a weathering profile varying from bedrock at the base upward through coarse and fine saprolites, and capped by a mottled zone and a lateritic colluvial nodular horizon. Chemical analyses and mass-balance calculations suggest that progressive weathering of the parent rock is characterized by an enrichment of Fe, Co, and Mn, a segregation of Ni at the boundary between the bedrock and the coarse sapolite and in the lower part of the fine saprolite, and a depletion of Mg, Ca, Si, Al, and Cr. The higher concentration of transition metals at the interface between the coarse and fine saprolite is due to vertical transfer and precipitation at the base of the weathering profile. In such a lateritic environment, the Pt-bearing chromite grains are progressively dissolved and the Pt-group minerals (PGM) are released in the weathering mantle with a preferential depletion of Pd with regard to Pt.

Keywords: Lateritic weathering, ultramafic rocks, mass-balance calculation, Pt-chromite, New Caledonia

Introduction

Lateritic weathering of rocks is one of the major processes that modify the Earth's surface and contribute to the geochemical cycle of elements (Marker et al. 1991; Compton et al. 2003). It affects numerous regions of the intertropical zone (Pedro 1968; Nahon 1986; Tardy and Roquin 1992; Tardy 1997), where long-term chemical weathering has led to the dissolution of primary minerals—including heavy minerals like metal-bearing spinel—resulting in supergene formation and accumulation of secondary and residual minerals in profiles 10–100 m thick. The mobilization and recycling of chemical elements during supergene weathering processes is complex, depending on dissolution kinetics of primary minerals, formation of secondary phases, Eh-pH conditions, mass transfers, and co-precipitation and ionic exchanges between various minerals (Harris and Adams 1966; Nesbitt 1979; Cramer and Nesbitt 1983; Nahon 1991; Nesbitt and Wilson 1992; Islam et al. 2002). We report here the chemical weathering of ultramafic rocks of New Caledonia and particularly the supergene dissolution of Pt-bearing chromite grains disseminated in the weathering profile to characterize the weathering processes of the parent rocks and the release mechanism of Pt-group minerals (PGM) in the weathering profile.

More than one-third of the area of New Caledonia is covered by ultramafic rocks, which are remnants of a Late Eocene overthrust belt now dissected by erosion (Paris 1981). These ultramafic rocks are deeply weathered, resulting in progressive leaching of Mg and Si and relative concentration of Fe and other metals in thick weathering profiles (Trescases 1975; Latham 1986). Ultramafic rocks are mainly harzburgite or lherzolite, which can exhibit serpentinization at their base, and are intercalated locally with dunite layers (Trescases 1975). Chromium spinel $(Mg,Fe^{2+})(Cr,Al,Fe^{3+})_2O_4$ is present interstitially in amounts up to 3% (Guillon 1975) or in pure chromite deposits of the ophiolitic harzburgites (Cassard et al. 1981; Augé 1985; Leblanc 1995). This primary chromite has been mobilized in eluvial and alluvial deposits. Significant proportions of this mineral have been previously reported in New Caledonian ophiolitic complexes, but the secondary supergene evolution of Cr-rich spinel is poorly understood (Phan and Routhier 1964). A petrological and geochemical study of lateritic weathering profiles can contribute to improving this knowledge, and, more particularly, to addressing the specific metallogenic issue of the supergene weathering processes of Pt-bearing chromite.

* E-mail: beauvais@cerege.fr

0003-004X/08/0001–022$05.00/DOI: 10.2138/am.2008.2605

GEOLOGICAL SETTING

The study area is located in the downslope part of the Pirogues River drainage basin in southern New Caledonia (Fig. 1). The lithological units of this area consist of ultramafic rock: cumulates of dunite, wehrlite, and pyroxenite, and also harzburgites, which are serpentinized and crosscut by pyroxenite dikes (Fig. 1). Platiniferous chromite grains are primarily concentrated either as stratiform accumulations in dunite and wehrlite or are disseminated in wehrlite and pyroxenite dikes. Most of the PGM are included in chromite (Augé and Maurizot 1995). Chromite forms thin schlieren and layers a few centimeters thick and a meter or so long in dunite and wehrlite cumulates. Irregular concentrations of massive chromite form ore in the pyroxenite dikes (Augé and Maurizot 1995). Chromite is found between large grains of pyroxene. Massive chromitite was also observed in the different horizons of the weathering profiles. The ultramafic rocks are deeply weathered under the influence of a warm and humid climate characterized by a mean annual rainfall of 1700 mm, with a wet season occurring from December to August. The ultramafic bedrock is generally overlain by a thick lateritic weathering mantle typically consisting of, from the base to the top (Trescases 1975; Besset 1980; Latham 1986; Llorca 1986): (1) a coarse saprolite comprised of parent rock blocks, surrounded by weathering cortices; (2) a fine saprolite where the silicates are totally hydrolyzed but the parent rock structure is preserved; (3) a mottled zone composed of some ferruginous nodules embedded in a goethitic matrix crossed by numerous millimeter-scale bioturbations; (4) a soft nodular layer consisting mainly of millimeter- to centimeter-sized nodules and pisoliths, and ferricrete fragments embedded in a red goethitic ferruginous matrix; and (5) a ferricrete exhibiting a massive, alveolar, and/or pisolitic structure, which is essentially composed of goethite and hematite. The parental structures are generally blurred in the ferruginous upper horizons.

Natural weathering profiles exposed in deep gullies (locally called "lavakas") have been described and sampled in situ (Fig. 2) for mineralogical and geochemical studies.

MATERIAL AND METHODS

Fourteen samples of parent rock, laterite, and soil were collected in situ for measurement of the bulk and grain density (Figs. 2 and 3). These samples were analyzed to determine (1) major-element composition by inductively coupled plasma-atomic emission spectroscopy (ICP-AES), and (2) trace and precious metals by inductively coupled plasma-mass spectrometry (ICP-MS). For ICP-AES analyses, the samples were crushed and finely ground (≤75 μm) after oven drying to be decomposed with 10 times their weight of a composite flux comprising 65% metaborate and 35% tetraborate according to the ME-ICP93 analytical procedure developed by the Australian Laboratory Services (ALS, Chemex). The resulting melts were dissolved in dilute nitric acid. Repeated fusion of finely ground powder was necessary to obtain complete decomposition of chromite, particularly for the samples containing coarser-grained chromite. For ICP-MS analysis of precious metals (Pt and Pd), each ground sample was fused with a mixture of lead oxide, sodium carbonate, borax, and silica, inquarted with 6 mg of gold-free silver and then coupled to yield a precious metal bead according to the PGM-MS23 analytical procedure developed by ALS Chemex, Australia. After

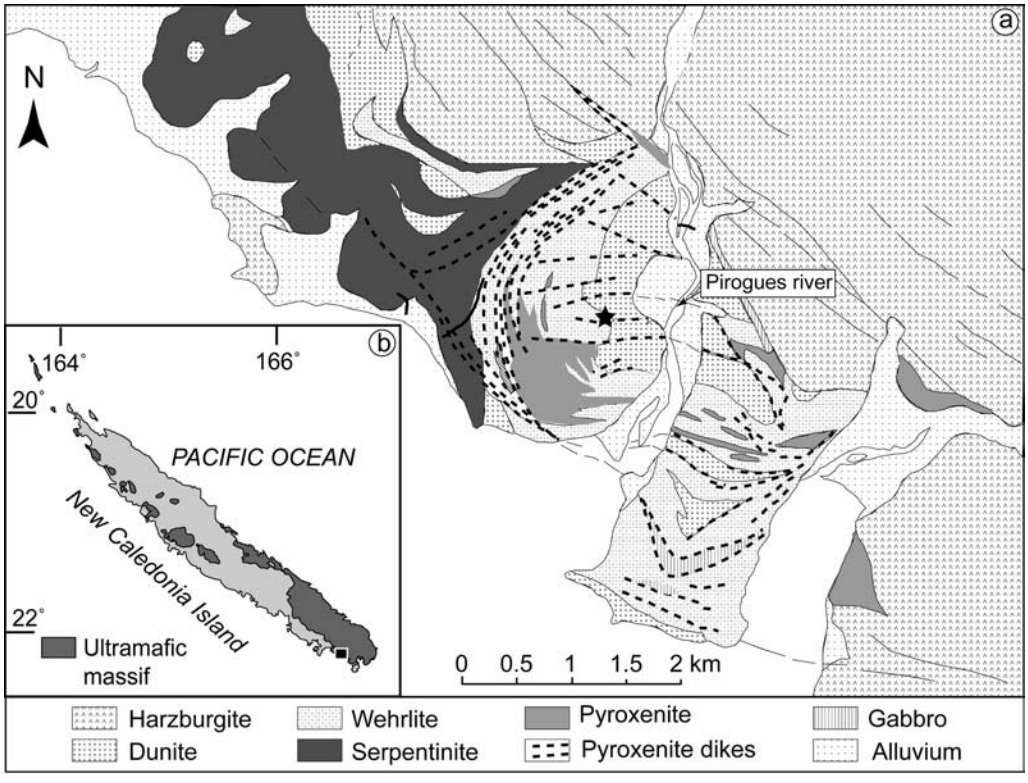

FIGURE 1. (**a**) Geological map and location of studied area (after Augé and Maurizot 1995). The black star shows the location of the studied weathering profile (Fig. 2). (**b**) Inset of the main Island of New Caledonia with its ultramafic massifs and location of **a** by the black rectangle.

cupellation, the bead was dissolved in nitric and hydrochloric acids and the solution diluted to volume. Detection limits for Pd and Pt are 1 and 0.5 ppb, respectively. X-ray diffraction (XRD) determinations were also obtained on each sample. Semi-quantitative proportions of minerals were deduced from measurements of the peak area of main peaks in XRD spectra.

Three samples of 50 kg each were collected in the friable layers of the weathering profile (fine saprolite, mottled zone, and nodular layer). The samples were carefully washed, sifted to 1 mm, and panned to separate out the heaviest particles. Chromite grains were separated from the other heavy minerals under a binocular microscope for morphological examination by scanning electron microscopy (SEM). After SEM observation, chromite grains were mounted with resin and polished sections were prepared for electron microprobe analyses. Microanalyses of chromite grains were obtained using a Cameca SX 100 electron microprobe at CREGU (Nancy, France) with an accelerating potential of 15 kV, a beam current of 50 nA, and a counting time of 10 s. The standards used were olivine for Mg, albite for Al, hematite for Fe, orthoclase for Si, Cr_2O_3 for Cr, $MnTiO_3$ for Mn and Ti, NiO-466.6 for Ni, ZnO for Zn, and synthetic Co for Co.

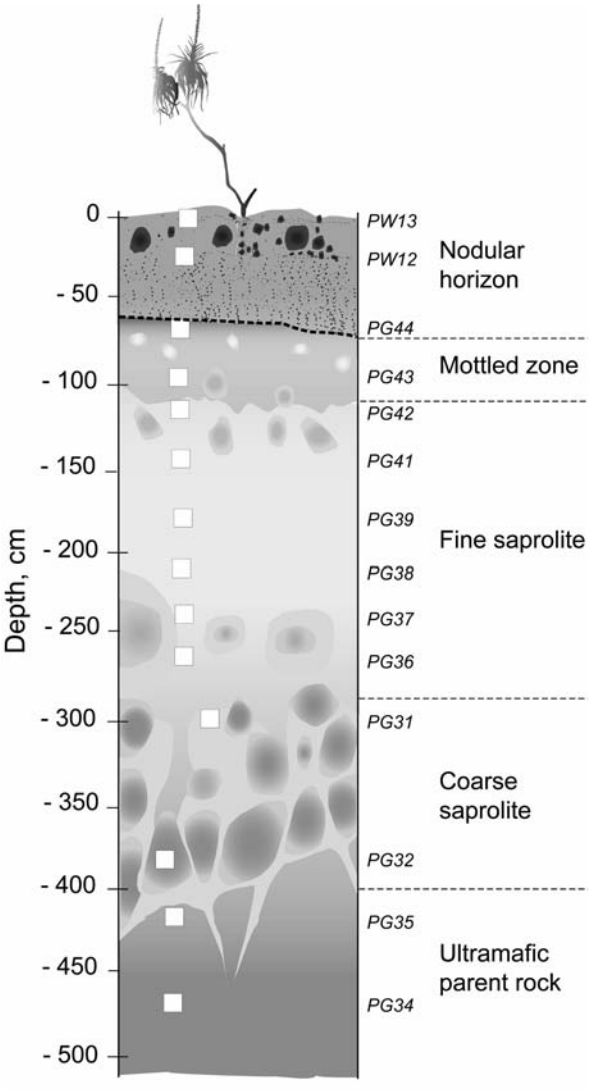

Figure 2. Weathering profile log from a crosscut into a natural gully ("lavaka") and the location of analyzed samples (white squares), the numbers of which being in italics.

Results and discussion

Physical and geochemical characterization

Density and porosity change. The weathering profile is developed on a wehrlite-type ultramafic rock (40–70% olivine, 30–45% antigorite, and 10–20% diopside), and its thickness is up to 4 m. At the base of the profile (Fig. 2), the greenish-black parent rock (–470 to –400 cm) changes to a brownish coarse saprolite (–400 to 290 cm) that preserves parental rock structure and texture. Above this zone (from –290 to –100 cm), a yellow fine saprolite is overlain by a red mottled zone (–100 to –60 cm) followed by a colluvial nodular horizon close to the ground surface (Fig. 2), that consists of ferruginous nodules, pisolites, and fragments of a previous ferricrete.

Rock porosity is an important physical parameter of weathering mantles as it controls soil, water, and air circulation, and thus permeability. Therefore, pores are a first-order factor controlling erosion and mass movement processes. In the profile studied, the bulk density decreases from an average 2.37 g/cm^3 in the fresh wehrlite to 1.32 g/cm^3 in the coarse saprolite, 0.93 and 1.13 g/cm^3 in the fine saprolite and mottled zone, respectively, and 1.71 g/cm^3 in the nodular horizon (Fig. 3a and Table 1). The grain density slightly increases from an average 3.05 g/cm^3 in the parent rock and the coarse saprolite, to 3.58 g/cm^3 in the fine saprolite and 3.64 g/cm^3 in the mottled zone, to 3.67 g/cm^3 in the nodular horizon (Fig. 3b and Table 1). The porosity change is thus very important, from 22% in the fresh wehrlite to 56%, on average, in the coarse saprolite, 74% in the fine saprolite, 69% in the mottled zone, and 53% in the upper nodular layer (Fig. 3c and Table 1).

Petrologic and geochemical patterns. The XRD mineralogical characterization of each horizon composing the weathering profile indicates the presence of olivine, antigorite, diopside, and goethite with accessory chromite and orthopyroxene. In the saprolites, the silicates are progressively replaced by goethite, olivine being the first affected by weathering. The coarse saprolite is composed of 30% olivine (up to 50% in the parent rock), 40% antigorite (35% in the parent rock), 15% diopsite, and 15% goethite. The base of the fine saprolite is composed of 15% olivine, 5% antigorite, 10% diopside (15% in the parent rock), and 50% goethite. At the top of the fine saprolite, olivine, antigorite, and diopside are completely replaced by goethite, which reaches 100%. The mottled zone and the nodular layer are essentially composed of goethite with accessory hematite and chromite.

The geochemical analyses of the unweathered wehrlite indicate, on average, 39.6 wt% SiO_2, and 34.7 wt% MgO, and 19.3 wt% Fe_2O_3 (Table 1). Silica decreases to 21.2 wt% at the top of the coarse saprolite and MgO to 7.1 wt%. The contents of Fe_2O_3 increase, on average, from 19.3 to 45.2 wt%. Aluminum and chromium contents do not significantly change between parent wehrlite and coarse saprolite: on average, 0.6–0.7 wt% Al_2O_3, 1.5–2.3 wt% Cr_2O_3. The transition metal contents increase, on average, from 1.97 to 4.40 g/kg for Mn, 0.23 to 0.48 g/kg for Co, and 0.34 to 0.53 g/kg for Ni (Table 1).

The coarse saprolite is progressively transformed into a fine saprolite, in which the texture and the structure of the parent

Table 1. Physical and chemical characteristics of the parent rock, and the different layers of the weathering profile (ρ_w = bulk density; ρ_g = grain density)

	Uncertainty	Bedrock		Coarse saprolite				Fine saprolite				Mottled zone		Nodular horizon	
Sample no.		PG34	PG35	PG32	PG31	PG36	PG37	PG38	PG39	PG41	PG42	PG43	PG44	PW12	PW13
Depth (cm)		–470	–420	–380	–300	–270	–240	–210	–180	–140	–110	–95	–70	–25	0
ρ_w (g/cm³)	±0.1	2.38	2.36	1.68	0.97	0.91	0.91	0.95	0.96	0.93	0.93	0.98	1.28	1.69	1.73
ρ_g (g/cm³)	±0.1	3.06	3.04	3.02	3.11	3.39	3.84	3.47	3.45	3.70	3.65	3.60	3.68	3.65	3.69
Porosity (%)		22.22	22.37	44.37	68.81	73.16	76.30	72.62	72.17	74.86	74.52	72.78	65.22	53.70	53.12
SiO_2 (wt%)	±0.01	39.48	39.81	34.65	21.27	6.00	4.08	3.32	2.99	2.20	2.07	2.09	1.88	2.10	1.90
Al_2O_3 (wt%)	±0.01	0.68	0.58	0.56	0.97	0.67	1.09	1.02	0.75	1.17	0.80	2.43	0.95	4.30	4.20
Fe_2O_3 (wt%)	±0.01	19.89	18.86	33.78	56.79	75.11	76.14	77.46	77.33	78.36	78.49	75.82	78.01	76.59	76.59
CaO (wt%)	±0.01	0.34	0.36	0.14	0.14	0.07	0.02	0.05	0.05	0.03	0.05	0.02	0.03	0.01	0.02
MgO (wt%)	±0.01	34.36	35.19	22.97	7.17	1.47	1.26	0.67	0.60	0.65	0.49	0.42	0.38	0.27	0.21
Cr_2O_3 (wt%)	±0.01	1.54	1.45	1.82	2.88	2.14	3.56	2.84	3.62	4.06	3.76	4.85	4.42	2.05	2.01
LOI (wt%)	±0.01	3.02	3.91	5.97	8.99	11.41	10.86	11.48	11.66	10.95	11.68	11.84	11.86	12.35	12.45
Total		99.31	100.16	99.89	98.21	96.87	97.01	96.84	97.00	97.42	97.34	97.47	97.53	97.67	97.38
Mn (mg/kg)	±100	2012	1935	3483	5340	8127	8359	8359	7817	8282	9365	8514	9365	9690	9790
Co (mg/kg)	±0.5	215	253	399	577	3140	2730	3080	3010	2670	2270	1950	1140	933	901
Ni (mg/kg)	±5	2910	4040	4230	6430	11100	9190	8250	8820	6140	5960	6760	5530	5598	4802
Pd (µg/kg)	±1	16	15	17	22	20	17	23	28	25	48	48	25	20	20
Pt (µg/kg)	±0.5	227	206	204	647	527	440	483	497	442	683	497	241	225	196
Pt/Pd		14.18	13.75	12.00	29.43	26.37	25.90	21.00	17.74	17.68	14.23	10.35	9.68	11.25	9.80

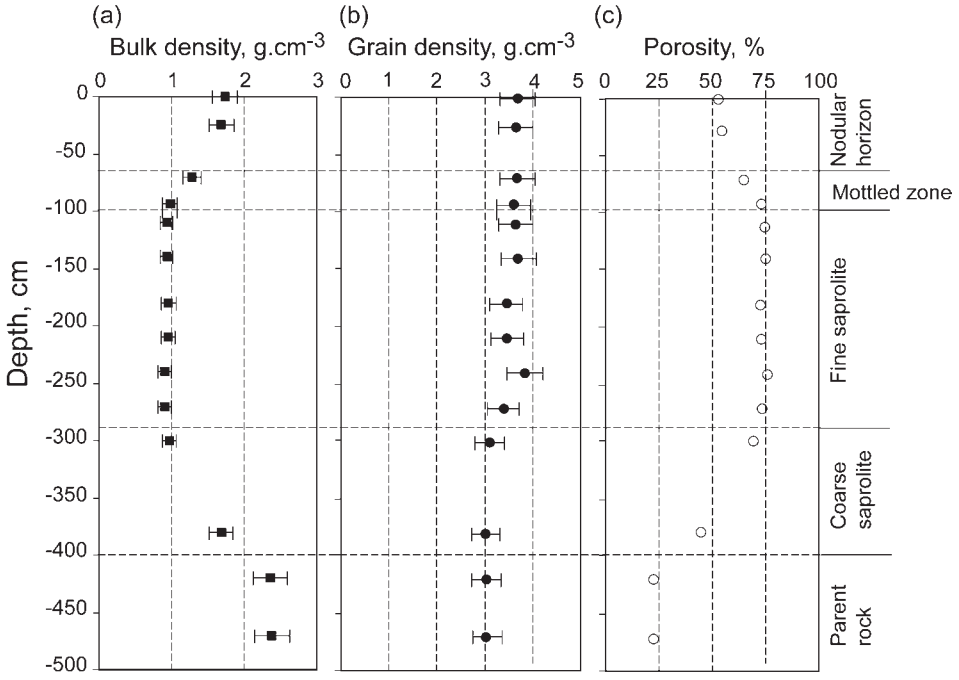

Figure 3. (**a**) Bulk density, (**b**) grain density, and (**c**) porosity variation along the profile.

rock are still preserved. On average, the geochemical analyses of the fine saprolite indicate 3.4 wt% SiO_2, 0.9 wt% Al_2O_3, 77 wt% Fe_2O_3, 3.3 wt% Cr_2O_3, 0.04 wt% CaO, 0.85 wt% MgO, 8.3 g/kg Mn, 2.8 g/kg Co, and 8.2 g/kg Ni (Table 1).

Toward the top of the profile, the fine saprolite changes to a bioturbated-mottled laterite in which the original rock structure is no longer preserved. The chemical composition is similar to the one analyzed in the upper part of the fine saprolite except for decreased Co content (Table 1).

Mass-balance calculations

Mass-balance calculations related to weathering processes require the application of rigorous means to estimate losses or gains based on a thorough petrological study (Millot and Bonifas 1955; Gresens 1967; Brimhall and Dietrich 1986; Colin et al. 1992, 1993; Beauvais and Colin 1993). The parental rock structures are well preserved in the saprolite suggesting that weathering processes have preserved the original volume. Based on the assumption that the volume has not varied between bedrock (–470 cm) and the top of the fine saprolite (–110 cm), isovolume mass-balance calculations can be applied to quantify mass transfers induced by the transformation of parent-rock into saprolite (Millot and Bonifas 1955). Numerous authors have mathematically formalized mass-balance calculations (Gresens 1967; Brimhall and Dietrich 1986) by a functional form of the constitutive relationships between the chemical compositions of parent and weathered material, their bulk densities, and volumes. The net gains and losses of chemical constituents

are calculated from the following equation (Brimhall and Dietrich 1986):

$$K_j = \left[\left(\frac{C_{jw} \times \rho_{jw}}{C_{jp} \times \rho_{jp}}\right) - 1\right] \times 100 \quad (1)$$

where K_j is the gain and/or loss factor of chemical element j ; C_{jw} and C_{jp} are the concentrations of chemical element j (expressed in g/kg for Si, Al, Fe, Ca, Mg, and Cr, or mg/kg for Mn, Co, and Ni) in the weathered layer, w, and the parent material, p, respectively; and ρ_{jw} and ρ_{jp} are bulk densities of the weathered material, w, and the parent material, p, respectively (expressed in g/cm^3).

The total mass (m_{jw}) of each element j gained or lost during the weathering process is calculated from the following equation (Colin et al. 1993):

$$m_{jw} = C_{jp} \times \rho_{jp} \times V_p \times K_{jw}, \quad (2)$$

where V_p is the volume of the parent rock ($V_p = 1m^3$), K_{jw} is the gain and/or loss factor of chemical element j in the weathered layer, w, calculated from the Equation 1, and C_{jp}, ρ_{jp}, and m_{jw} are expressed in kg/ton, ton/m^3, and kg/m^3, respectively.

Mass-balance calculations show that 96% of Si, 99% of Mg, and 94% of Ca have been depleted in the fine saprolite (Table 2a and Fig. 4) that corresponds, on average, to mass transfers of –426 kg Si, –488 kg Mg, and –5.4 kg Ca per cubic meter of weathered parent rock (Table 2b). This is accompanied, on average, by 47% loss of Al, and 16% loss of Cr, i.e., –4 kg/m^3 Al and –4 kg/m^3 Cr, the highest values being recorded at the base of the fine saprolite (Table 2, Figs. 4a and 4c). Iron, Mn, and Co contents are enriched at the top of the coarse saprolite only by 4.7% (+17.2 kg/m^3), 8% (+0.39 kg/m^3), and 9% (+0.05 kg/m^3), respectively, whereas Ni is slightly depleted by –10% (–0.69 kg/m^3) (Fig. 4, Table 2). At the base of the fine saprolite, the enrichment rates strongly increase by 30% (+110 kg/m^3) for Fe, 45% (+3.18 kg/m^3) for Ni, 54% (+2.61 kg/m^3) for Mn, and 458% (+2.35 kg/m^3) for Co. At the top of the fine saprolite, the enrichment rates are 38% (+142 kg/m^3) for Fe, 81% (+3.9 kg/m^3) for Mn, and 312% (+1.6 kg/m^3) for Co, whereas Ni is depleted by –20% (–1.38 kg/m^3) (Tables 2a and 2b).

The sharp decrease of Si, Mg, and Ca contents (from parent rock to saprolite) reflects the congruent weathering of primary silicates (Eggleton et al. 1987; Nesbitt and Wilson 1992; Islam et al. 2002). The weathering creates high porosity and resultant improved drainage conditions if pore spaces are interconnected (Trescases 1975; Latham 1986; Marker et al. 1991). The Fe-enrichment at the transition between coarse and fine saprolite (Fig. 4a, Table 2) is due to relatively short vertical migrations of Fe in the weathering profile that has led to goethite formation, which may have trapped transition metals such as Mn, Co, and Ni (Millot and Bonifas 1955; Tardy and Roquin 1992; Beauvais and Colin 1993; Beauvais and Roquin 1996).

The primary host minerals for Ni in the ultramafic rocks are olivine, serpentine, and accessory pyroxene (Zeissink 1969; Trescases 1975; Besset 1980; Colin et al. 1990; Gaudin 2002). During the weathering of these parent minerals under strongly oxidizing conditions, Ni is mobilized and enriched by co-precipitation with secondary Fe and Mn oxides at the transition between the coarse and fine saprolite (Fig. 4c, Table 2) as previously shown (Schellmann 1981; Golightly 1981; Elias et al. 1981; Trescases 1975; Reimann and Caritat 1998).

Manganese enrichment in the fine saprolite (on average, +60%), as compared to its content in the parent rock (Table 2a), can be explained by significant vertical and/or lateral transfer of Mn, which is released as Mn^{2+} in the saturated zone of the deeper saprolite (Golightly 1979). Vertical transfer may be due to the leaching of Mn from the near-surface part of the profile under conditions of low pH and high CO_2 activity. These environmental conditions favor reduction of Mn^{4+} to Mn^{2+} (Golightly 1979; Beauvais et al. 1987). Colloidal Mn^{2+} complexes are highly mobile and can be transported in the soils over long distances (Krauskopf 1979; Marker et al. 1991). As soon as Mn-bearing solutions reach the lower part of the weathering profile, rising

TABLE 2. Results of (**a**) the mass balance factor (K) and (**b**) the total mass transfer (m) of chemical elements calculated from Equations 1 and 2, respectively

	Bedrock		Coarse saprolite		Fine saprolite					
Sample	PG34	PG35	PG32	PG31	PG36	PG37	PG38	PG39	PG41	PG42
Depth (cm)	–470	–420	–380	–300	–270	–240	–210	–180	–140	–110
(**a**)										
K_{Si} (%)	0.00	–0.01	–38.05	–78.04	–94.19	–96.05	–96.64	–96.95	–97.82	–97.95
K_{Al} (%)	0.00	–15.42	–41.87	–41.86	–62.33	–38.71	–40.13	–55.51	–32.77	–54.03
K_{Fe} (%)	0.00	–5.98	7.85	4.69	29.89	31.67	39.84	41.08	38.49	38.72
K_{Ca} (%)	0.00	4.99	–70.93	–83.22	–92.13	–97.75	–94.13	–94.07	–96.55	–94.25
K_{Mg} (%)	0.00	1.55	–52.81	–91.50	–98.36	–98.60	–99.22	–99.30	–99.26	–99.44
K_{Mn} (%)	0.00	–4.65	22.17	8.16	54.41	58.82	65.80	56.69	60.81	81.85
K_{Cr} (%)	0.00	–6.64	–16.58	–23.78	–46.87	–11.61	–26.39	–5.18	3.02	–4.59
K_{Ni} (%)	0.00	37.66	2.61	–9.94	45.85	20.75	13.16	22.26	–17.55	–19.97
K_{Co} (%)	0.00	16.69	31.00	9.38	458.41	385.50	471.82	464.71	385.26	312.57
(**b**)										
m_{Si} (kg/m^3)	0.00	–0.05	–166.95	–342.45	–413.31	–421.47	–424.08	–425.40	–429.25	–429.81
m_{Al} (kg/m^3)	0.00	–1.32	–3.58	–3.58	–5.34	–3.31	–3.44	–4.75	–2.81	–4.63
m_{Fe} (kg/m^3)	0.00	–21.98	28.87	17.24	109.95	116.50	146.56	151.10	141.58	142.42
m_{Ca} (kg/m^3)	0.00	0.29	–4.10	–4.81	–5.32	–5.65	–5.44	–5.43	–5.58	–5.45
m_{Mg} (kg/m^3)	0.00	7.67	–260.42	–451.18	–485.05	–486.20	–489.28	–489.64	–489.47	–490.37
m_{Mn} (kg/m^3)	0.00	–0.22	1.06	0.39	2.61	2.82	3.15	2.72	2.91	3.92
m_{Cr} (kg/m^3)	0.00	–1.66	–4.16	–5.96	–11.75	–2.91	–6.62	–1.30	0.76	–1.15
m_{Ni} (kg/m^3)	0.00	2.61	0.18	–0.69	3.18	1.44	0.91	1.54	–1.22	–1.38
m_{Co} (kg/m^3)	0.00	0.09	0.16	0.05	2.35	1.97	2.41	2.38	1.97	1.60

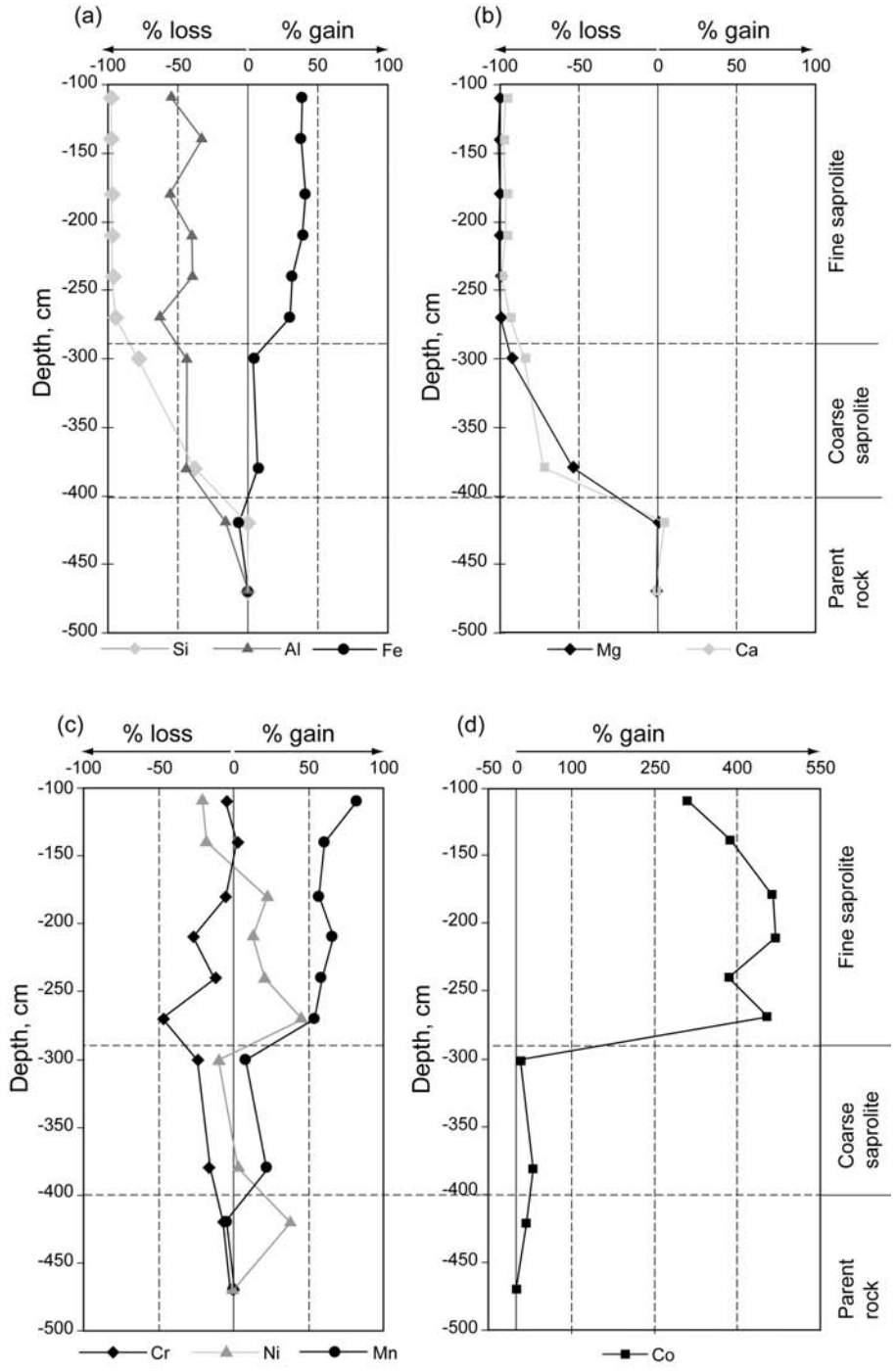

FIGURE 4. Results of the geochemical mass-balance calculation along the profile.

pH (due to silicate hydrolysis) and increased concentration of the solution above the saprolite are likely to result in the oxidation of Mn^{2+} and precipitation of Mn oxides from the colloidal solution (Trescases 1975; Golightly 1979; Llorca 1986; Marker et al. 1991).

The behavior of Co is also controlled by physical-chemical properties of the downward-migrating solutions (Marker et al. 1991). Cobalt is adsorbed by negatively charged Mn^{4+} colloids and/or incorporated into Mn oxides (Burns 1976; Manceau et al. 1987; Llorca and Monchoux 1991; Llorca 1993). Precipitation of Co at the base of the profile, where pH is higher, is more effective because the solubility product of Co hydroxide is lower than that of Mn hydroxide (Trescases 1975; Schellmann 1978; Golightly 1981). This property can explain the higher enrichment factor of Co (+450%) compared to Mn (+54%) or Ni (+45%) in the lower cementation zone (Figs. 4c and 4d, Table 2) (Marker et al. 1991).

The Cr-bearing minerals in the ultramafic rocks are mainly chromite and accessory silicates. Chromium-bearing silicate minerals are, however, depleted in the upper saprolite. Some Cr may be leached downward in the form of $Cr(OH)_3$ in alkaline environments (Marker et al. 1991). Chromium within chromite is generally considered immobile in supergene environments (Trescases 1975; Schellmann 1978; Becquer et al. 2003). However, thermodynamic and field studies have shown that chromite is soluble in lateritic environments (Fendorf 1995), suggesting that Cr in laterites derived from the weathering of ultramafic rocks may be depleted from the profile. As chromite is the main host mineral of Al in the wehrlite, its solubility also explains the depletion of Al in the profile.

Supergene dissolution of chromite

The chemical compositions of chromite from different samples of Pt-rich chromitite of the Pirogues site are plotted in Figure 5. Also shown are compositions of disseminated chromite from the cumulate series, and chromitite from previously studied mantle deposits (Augé and Maurizot 1995) such as those from the Tiebaghi massif in northwestern New Caledonia, in which the chromite has a very constant composition [high Cr^{3+} (55.5–63.5 wt% Cr_2O_3) and low Fe^{3+} (1.5–4.3 wt% Fe_2O_3)]. Chromite disseminated in mineralized cumulates is slightly impoverished in Cr (Fig. 5). Platinum-bearing chromite concentrations in the cumulate series of the Pirogues area differ significantly from those of mantle chromitite in having relatively low Cr^{3+} (40–46 wt% Cr_2O_3) and high Fe^{3+} (10–17 wt% Fe_2O_3) (Fig. 5). No significant difference was observed between chromitite of pyroxenite dikes and chromitite of cumulates.

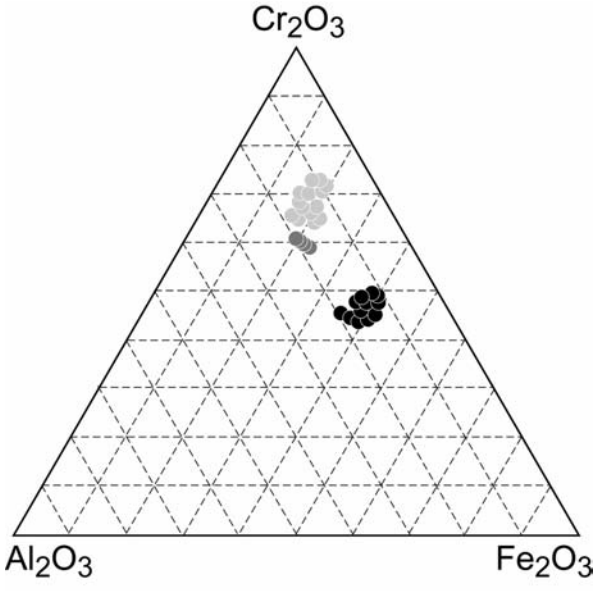

Figure 5. Chemical compositions of chromite from PGE-rich chromitite of the Pirogues River mineralization (black circles) and disseminated chromite in cumulate rocks hosting the mineralization (gray circles). Light-gray circles correspond to mantle chromitite from Tiébaghi (after Augé 1985).

The progressive weathering of chromite is illustrated in Figure 6. The Pt-bearing chromite in the parent rock and coarse saprolite is euhedral (Fig. 6a), with surfaces that may represent small primary dissolution cracks (Fig. 6b). In the fine saprolite, where the lowest bulk densities and the highest porosities were measured (Fig. 3, Table 1), the dissolution of chromite starts along the primary cracks and increases until forming a network of etch pits of sub-micrometric size (Figs. 6c and 6d). This effectively corresponds to the highest losses of Cr (Fig. 4c, Table 2). In the mottled zone, residual chromite grains with smooth edges

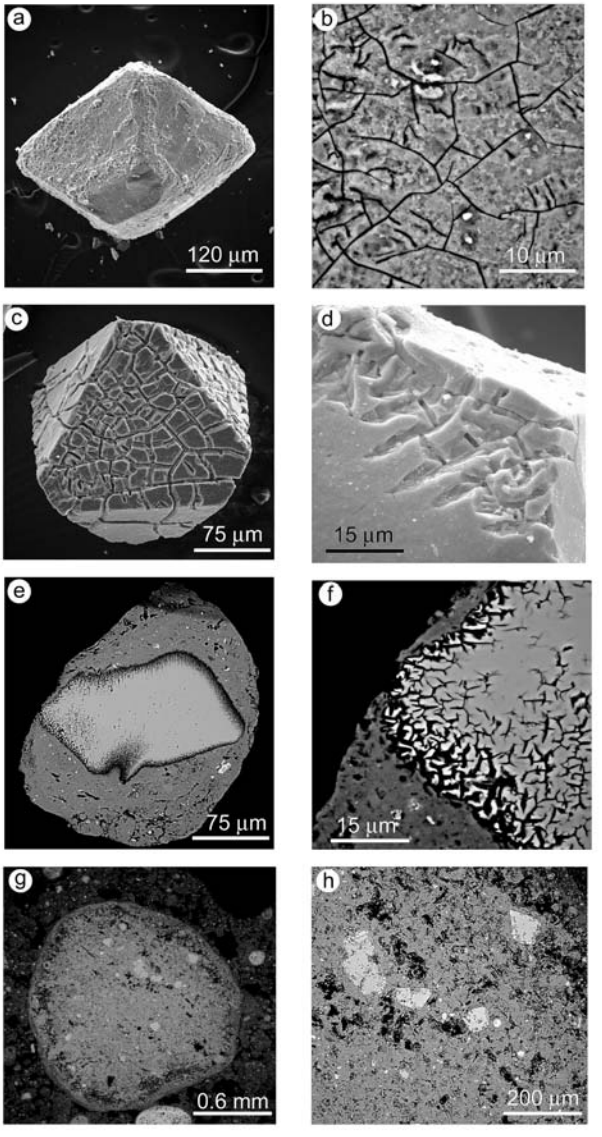

Figure 6. SEM images of the progressive weathering of chromite (**a**) euhedral grain of primary chromite in the coarse saprolite, (**b**) detail of a primary chromite grain surface showing dissolution cracks, (**c**) euhedral grain of chromite affected by a microdrain network in the red laterite, (**d**) etching dissolution pits of a chromite grain, (**e**) residual chromite grain in a ferruginous cortex, (**f**) detail of dissolution features of a chromite, (**g**) small size chromite grain disseminated in a pisolite, and (**h**) detail of **g**.

are embedded in ferruginous aggregates and/or pisolites (Fig. 6e), which are essentially composed of goethite. The dissolution front increases in the chromite by widening of microcracks and fissures hosting weathering solutions (Fig. 6f). The supergene dissolution process leads to the dislocation of chromite crystals in the superficial layers (Figs. 6g and 6h). Chromite grain dissolution in supergene environments is driven by an hydrolysis process that produces $Cr(OH)_3$ (Cooper 2002) via:

$$FeCr_2O_4 + 2H_2CO_3 + 2H_2O = Fe^{2+}_{aq} + 2Cr(OH)_3 + 2HCO^-_3 \quad (3)$$

The production of $Cr(OH)_3$ requires moist, slightly reduced conditions to keep Fe^{2+} ions in solution, such as those prevailing in the fine saprolite, which is characterized by an unconnected fine porosity and poor drainage. The $Cr(OH)_3$ thus produced can be adsorbed on to the surface of the crystal structure of Fe and/or Mn oxyhydroxides (McKenzie 1977; Manceau and Charlet 1992; Fendorf 1995).

The dissolution reaction of $Cr(OH)_3$ to produce soluble Cr^{3+} ions is represented by:

$$Cr(OH)_3 + 3H^+ = Cr^{3+}_{aq} + 3H_2O \quad (4)$$

This reaction is possible only under strongly acidic conditions with pH values lower than 4 (Fendorf 1995; Cooper 2002). Such conditions prevail at the top of lateritic profiles, which is commonly rich in organic matter.

The poorly aerated chromite-rich ferruginous aggregates can also undergo oxidation-reduction conditions that favor the hydrolysis of Cr^{3+} into $Cr(OH)_3$ (Cooper 2002). The dissolution of chromite ultimately leads to the release of PGM initially contained in chromite crystals.

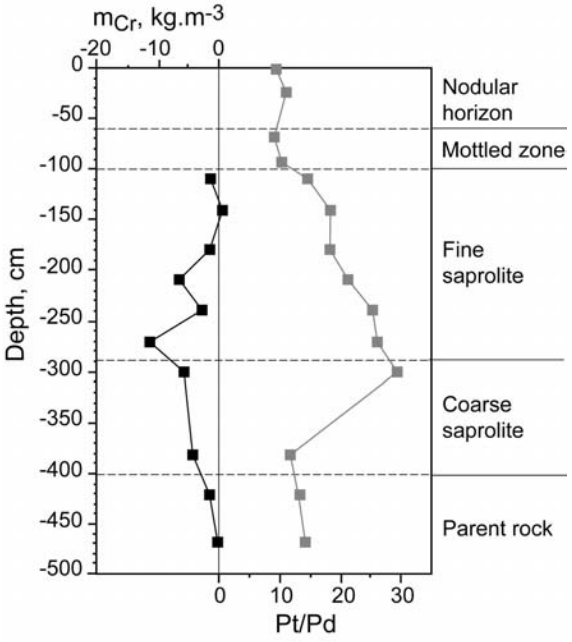

FIGURE 7. Comparison between the total mass transfer of Cr and Pt/Pd variation in the weathering profile.

Residual origin of platinum

Decoupling of platinum group elements, Pt and Pd, and variation of the ratio Pt/Pd, are characteristic of the behavior of the PGE in supergene environments (Prichard and Lord 1994; Evans et al. 1994; Oberthür et al. 2003). Between the bedrock and the upper part of the fine saprolite, the Pt/Pd ratio is the highest where Cr is most depleted (Fig. 7, Tables 1 and 2). The increase of Pt/Pd in the weathering profile reflects the preferential release of Pd compared to Pt (Varajao et al. 2000). Figure 7 also suggests that PGM could be released concomitant with chromite dissolution, and also, that the supergene dissolution of Pt-bearing chromite and/or newly released PGM lead to a preferential depletion of Pd with regard to Pt. The specific behavior of PGM in the lateritic weathering profile is addressed separately (Traoré et al. 2008).

CONCLUDING STATEMENT

This investigation documents the geochemical mass balance of ultramafic rock weathering and particularly the supergene dissolution of Cr-rich spinel. Our results demonstrate the decoupling of Pt-group elements and Cr during the lateritic weathering of Pt-bearing chromite and suggest that the Pt mineralization is everywhere residual. These findings can be useful in the geochemical prospecting for Cr and Pt deposits in tropical environments.

ACKNOWLEDGMENTS

This work is a contribution IRD-UMR161-CEREGE. P. Maurizot is thanked for introducing us to the study area. Michel Cathelineau, Gaëlle Bouichet, Marc Brouand, and Philippe Larqué are gratefully acknowledged for their help during mineralogical investigations. J. Butscher, D. Chardon, V. Chevillotte, V. Combier, A. Paugam, J. Perrier, N. Perrier, and B. Robineau are also thanked for their help during fieldwork. Giorgio Garuti, Anthony Velbel, and an anonymous reviewer are thanked for their helpful review of the manuscript.

REFERENCES CITED

Augé, T. (1985) Chromite et minéraux du groupe du platine dans les complexes ophiolitiques. Caractérisation des séries hôtes, 270 p. Ph.D. thesis, Université Orléans, France.

Augé, T. and Maurizot, P. (1995) Stratiform and alluvial platinum mineralization in the New Caledonia ophiolite complex. Canadian Mineralogist, 33, 1023–1045.

Beauvais, A. and Colin, F. (1993) Formation and transformation processes of iron duricrust systems in tropical humid environment. Chemical Geology, 106, 77–101.

Beauvais, A. and Roquin, C. (1996) Petrological differentiation patterns and geomorphic distribution of ferricretes in Central Africa. Geoderma, 73, 63–82.

Beauvais, A., Melfi, A.J., Nahon, D., and Trescases, J-J. (1987) Pétrologie du gisement latéritique manganesifère d'Azul (Brésil). Mineralium Deposita, 22, 124–134.

Becquer, T., Quantin, C., Sicot, M., and Boudot, J.P. (2003) Chromium availability in ultramafic soils from New Caledonia. Science of Total Environment, 301, 251–261.

Besset, F. (1980) Localisation et répartitions successives du nickel au cours de l'altération latéritique des péridotites de Nouvelle-Calédonie. Mémoire du Centre d'Etudes et de Recherches Géologiques et Hydrologiques, 129 p., Tome XV, CERGA Ed., Montpellier, France.

Brimhall, G.H. and Dietrich, W.E. (1986) Constitutive mass-balance relations between chemical composition, volume, density, porosity and strain in metasomatic hydrochemical systems: Results on weathering and pedogenesis. Geochimica et Cosmochimica Acta, 51, 567–587.

Burns, R.G. (1976) The uptake of cobalt into ferromanganese nodules, soils and synthetic manganese (IV) oxides. Geochimica et Cosmochimica Acta, 40, 95–102.

Cassard, D., Nicolas, A., Rabinovitch, M., Moutte, J., Leblanc, M., and Prinzhofer, A. (1981) Structural classification of chromite pods in southern New Caledonia. Economic Geology, 76, 805–831.

Colin, F., Nahon, D., Trescases, J.J., and Melfi, A.J. (1990) Lateritic weathering of pyroxenites at Niquelandia, Goias, Brazil: The supergene behavior of nickel. Economic Geology, 85, 1010–1023.

Colin, F., Brimhall, G.H., Nahon, D., Lewis, C.J., Baronnet, A., and Danti, K. (1992) Equatorial rain forest lateritic mantles: A geomembrane filter. Geology, 20, 523–526.

Colin, F., Veillard, P., and Ambrosi, J.P. (1993) Quantitative approach to physical and chemical gold mobility in equatorial rainforest lateritic environment. Earth and Planetary Science Letters, 114, 269–285.

Compton, J.S., White, R.A., and Smith, M. (2003) Rare earth element behavior in soils and salt pan sediments of a semi-arid granitic terrain in the Western Cape, South Africa. Chemical Geology, 201, 239–255.

Cooper, G.R.C. (2002) Oxidation and toxicity of chromium in ultramafic soils in Zimbabwe. Applied Geochemistry, 17, 981–986.

Cramer, J.J. and Nesbitt, H.W. (1983) Mass-balance relations and trace element mobility during continental weathering of various igneous rocks. In S.G. Memory, Ed., Symposium on Petrology of Weathering and Soils, p. 63–73.

Eggleton, RA., Foudoulis, C., and Varkevisser, D. (1987) Weathering of basalt: changes in rock chemistry and mineralogy. Clays and Clay Minerals, 35, 161–169.

Elias, M., Donaldson, M.J., and Giorgetta, N. (1981) Geology, mineralogy, and chemistry of lateritic nickel-cobalt deposits near Kalgoorlie, Western Australia. Economic Geology, 76, 1775–1783.

Evans, D.M., Buchanan, D.L., and Hall, G.E.M. (1994) Dispersion of platinum, palladium and gold from the main sulphide zone, Great Dike, Zimbabwe. Transactions of the Institution of Mining and Metallurgy, 103 (Section B: Applied Earth Science), B57–B67.

Fendorf, S.E. (1995) Surface reactions of chromium in soils and waters. Geoderma, 67, 55–71.

Gaudin, A. (2002) Cristallochimie des smectites du gisement latéritique nickélifère de Murrin Murrin (Ouest Australie), 236 p. Ph.D. thesis, Université Aix-Marseille III, France.

Golightly, J.P. (1979) Geology of Soroako nickeliferous laterite deposits. AIME International Laterite Symposium, New Orleans, U.S.A., p. 38–55.

——— (1981) Nickeliferous laterite deposits. Economic Geology, 75th Anniversary vol., p. 710–735.

Gresens, R.L. (1967) Composition-volume relations of metasomatism. Chemical Geology, 2, 47–65.

Guillon, J.H. (1975) Les Massifs péridotitiques de Nouvelle-Calédonie: type d'appareil ultrabasique stratiforme de chaine récente. Mémoire ORSTOM 76 Paris, 113 p.

Harris, R.C. and Adams, J.A.S. (1966) Geochemical and mineralogical studies on the weathering of granitic rocks. American Journal of Science, 264, 146–173.

Islam, M.R., Peuraniemi, V., Aario, R., and Rojstaczer, S. (2002) Geochemistry and mineralogy of saprolite in Finish Lapland. Applied Geochemistry, 17, 885–902.

Krauskopf, K.B. (1979) Introduction to Geochemistry, 617 p. McGraw-Hill, Tokyo.

Latham, M. (1986) Altération et pédogenèse sur roches ultrabasiques en Nouvelle-Calédonie: Genèse et évolution des accumulations de fer et de silice en relation avec la formation du modelé, 331 p. Etudes et Thèses, ORSTOM, Paris, France.

Leblanc, M. (1995) Chromitite and ultramafic rock compositional zoning through a paleotransform fault, Poum, New Caledonia. Economic Geology, 90, 2028–2039.

Llorca, S. (1986) Les concentrations cobaltifères supergènes en Nouvelle-Calédonie: Géologie, minéralogie, 90 p. Ph.D. thesis, Université Paul Sabatier, Toulouse, France.

——— (1993) Metallogeny of supergene cobalt mineralization, New Caledonia. Australian Journal of Earth Science, 40, 377–385.

Llorca, S. and Monchoux, P. (1991) Supergene cobalt minerals from New Caledonia. Canadian Mineralogist, 29, 149–161.

Manceau, A. and Charlet, L. (1992) X-ray absorption spectroscopic study of the sorption of Cr(III) at the oxide-water interface: I. Molecular mechanism of Cr(III) oxidation on Mn oxides. Journal of Colloidal Interface Science, 148, 425–442.

Manceau, A., Llorca, S., and Calas, G. (1987) Crystal chemistry of cobalt and nickel in lithiophorite and asbolane from New Caledonia. Geochimica et Cosmochimica Acta, 51, 105–113.

Marker, A., Friedrich, G., Carvalho, A., and Melfi, A. (1991) Control of the distribution of Mn, Co, Zn, Zr, Ti, and REEs during the evolution of lateritic covers above ultramafic complexes. Journal of Geochemical Exploration, 40, 361–383.

McKenzie, R.M. (1977) Manganese oxides and hydroxides. In J.B. Dixon and S.B. Weed, Eds., Minerals in Soil Environments, p. 181–193. Soil Science Society of America, Madison, Wisconsin.

Millot, G. and Bonifas, M. (1955) Transformations isovolumiques dans les phénomènes de latéritisation et de bauxitisation. Bulletin du Service de la Carte Géologique d'Alsace-Lorraine, Strasbourg, 8, 8–10.

Nahon, D.B. (1986) Evolution of iron crusts in tropical landscapes. In S.H. Coleman and D.P. Dethier, Eds., Rates of Chemical Weathering of Rocks and Minerals, p. 169–187. Academic Press Incorporation, San Diego.

Nahon, D. (1991) Introduction to the Petrology of Soils and Chemical Weathering, 313 p. Wiley Interscience, New York.

Nesbitt, H.W. (1979) Mobility and fractionation of rare earth elements during weathering of granodiorite. Nature, 279, 206–210.

Nesbitt, H.W. and Wilson, R.E. (1992) Recent chemical weathering of basalts. American Journal of Science, 292, 740–777.

Oberthür, T., Weiser, T.W., and Gast, L. (2003) Geochemistry and mineralogy of platinum-group elements at Hartley Platinum Mine, Zimbabwe. Mineralium Deposita, 38, 344–355.

Paris, J.P. (1981) Géologie de la Nouvelle-Calédonie: Un essai de synthèse, 278 p. Mémoire BRGM 113, Orléans.

Pedro, G. (1968) Distribution des principaux type d'altération chimique à la surface du globe. Présentation d'une esquisse géographique. Revue de Géographie Physique et Géologie Dynamique, 10, 457–470.

Phan, K.D. and Routhier, P. (1964) Altération météorique de chromite de Nouvelle-Calédonie: Etude à la microsonde électronique. Contribution à la géochimie supergène du chrome en milieu latéritique. Conséquences pratiques pour la concentration des chromite détritiques. Bulletin BRGM, 4, 111–133.

Prichard, M.H. and Lord, R.A. (1994) Evidence for differential mobility of platinum-group elements in the secondary environnement in Shetland ophiolite complex. Transactions of the Institution of Mining and Metallurgy, 103, (Section B; Applied Earth Science), B79–B86.

Reimann, C. and de Caritat, P.D. (1998) Chemical elements in the environment. Factsheets for the geochemist and environmental scientist. Springer Verlag Publication, Berlin.

Schellmann, W. (1978) Behavior of nickel, cobalt, and chromium in ferruginous lateritic nickel ores. Bulletin BRGM, 2, 275–282.

——— (1981) Formation of nickel silicate ores by weathering of ultramafic rocks. Development in Sedimentology, 35, 623–634.

Tardy, Y. (1997) Petrology of laterites and tropical soils, 459 p. Balkema, Amsterdam.

Tardy, Y. and Roquin, C. (1992) Geochemistry and evolution of lateritic landscapes. In I.P. Martini and W. Chesworth, Eds., Weathering, Soils and Paleosols, p 407–443. Elsevier Publication, Amsterdam.

Traoré, D., Augé, T., Beauvais, A., Parisot, J.C., Colin, F., and Cathelineau, M. (2008) Chemical and physical transfers in an ultramafic rock weathering profile: Part 2. Dissolution vs. accumultion of platinum group minerals. American Mineralogist, 93, 31–38.

Trescases, J.J. (1975) L'évolution géochimique supergène des roches ultrabasiques en zone tropicale: formation des gisements nickélifères de Nouvelle- Calédonie, 280 p. Mémoire ORSTOM 78, Paris.

Varajao, C.A.C., Colin, F., Vieillard, P., Melfi, A.J., and Nahon, D. (2000) Early weathering of palladium gold under lateritic conditions, Maquine Mine, Minas Gerais: Brazil. Applied Geochemistry, 15, 245–263.

Zeissink, H.E. (1969) The mineralogy and geochemistry of a nickeliferous laterite profile (Greenvale, Queensland, Australia). Mineralium Deposita, 4, 132–152.

Manuscript received February 13, 2007
Manuscript accepted September 4, 2007
Manuscript handled by Jennifer Thomson